ENEE662 Final Project

Convex Formulations for Antenna Array Pattern Optimization: LP, QP, and SOCP

Team Members:
Abu Horaira Hridhon, Jarin Tasnim, Nathan Daetwyler

ENEE 662: Convex Optimization – Fall 2025

The codes for this study are available at this Github repository.

1 Introduction

Antenna arrays play a central role in wireless communication, radar, and sensing systems due to their ability to shape and steer their electromagnetic radiation patterns [1, 2, 3]. By appropriately choosing the complex excitation weights applied to each antenna element, an array can concentrate energy in desired directions. This capability is fundamental to applications such as beamforming in massive MIMO systems, adaptive radar, and spatial filtering in congested spectral environments. Traditionally, phase-only control is utilized to steer the directivity of the array [4]. This technique involves fixed excitation magnitudes and direction-dependent phase shifts to form a main beam in the desired direction. While this approach is simpler and more widely used, adjusting only the phase limits the ability to control aspects that impede the performance of the antenna array. Such requirements include the ability to place nulls to reject interference and suppress sidelobe levels (SLLs). One alternative is adjusting both amplitude and phase in order to achieve the desired pattern.

The process of determining the excitation weights that yield a desired radiation pattern is known as antenna array pattern synthesis. Closed-form solutions can be derived from classical synthesis techniques, such as Dolph–Chebyshev and Taylor distributions. However, these approaches are often limited in their ability to incorporate multiple, simultaneous constraints such as arbitrary null placement, power control, or irregular array geometries. As a result, many practical array synthesis problems are inherently constrained optimization problems. Additionally, other optimization-based approaches have been widely explored. Even so, traditional formulations often rely on phase-only control or heuristic methods such as genetic algorithms and particle swarm optimization. While these methods can produce satisfactory designs in practice, they usually lead to nonconvex optimization problems and are computationally expensive [5, 6, 7].

In contrast, convex optimization yields efficient solutions and can guarantee global optimality [8]. By allowing both amplitude and phase control of the antenna excitations, the array pattern synthesis problem can be reformulated into standard convex optimization problems. Furthermore, the radiation pattern can be expressed using Hermitian quadratic forms, allowing the formulation of Linear Programs (LP), Quadratic Programs (QP), and Second-Order Cone Programs (SOCP).

In this project, we adopt a convex optimization technique for antenna array pattern synthesis, following the framework presented by Vaquero and Cócoles [9]. Our primary goal is to maximize directivity for a pre-specified array antenna geometry towards a desired direction while enforcing constraints on null placement and sidelobe levels. We first aim to replicate and verify

the proposed framework using tools and methods found in ENEE662 materials, and demonstrate how the proposed design constraints can be formed into convex optimization problems. We hope to illustrate how LP, QP, and SOCP formulations emerge from the same underlying physical model, and that global optimality of a given array antenna layout can be achieved.

2 Radiation Pattern Fundamentals

2.1 Pattern Multiplication

We begin by deconstructing the process in [9] for constructing convex problems from traditional antenna array equations found in combination from [9, 10]. For an array of identical radiating elements, the total far-field radiation pattern can be expressed using the principle of *pattern multiplication*. Specifically, the radiated electric field in the far zone can be written as

$$E(\theta, \phi) = E_e(\theta, \phi) \cdot AF(\theta, \phi), \tag{1}$$

where $E_e(\theta, \phi)$ denotes the radiation pattern of a single element placed at a reference location, and $AF(\theta, \phi)$ is the array factor [10]. This result follows directly from classical antenna theory and highlights that the spatial shaping capability of an array is governed by the array factor, which depends only on the geometry of the array and the complex excitation applied to each element.

In this work, we assume isotropic elements so that $E_e(\theta, \phi) = 1$ [9]. Under this assumption, the total radiation pattern is entirely determined by the array factor. This will allow the optimization problem to focus exclusively on excitation design rather than element-specific radiation characteristics, as we will show.

2.2 Array Factor Representation

Consider an array of N elements located at positions $\mathbf{r}_n = x_n\hat{\mathbf{x}} + y_n\hat{\mathbf{y}}$, $n = 1, \ldots, N$. Let $a_n \in \mathbb{C}$ denote the complex excitation of the nth element. The array factor can be written as

$$AF(\theta, \phi) = \sum_{n=1}^{N} a_n e^{jk(\mathbf{r}_n \cdot \hat{\mathbf{u}}(\theta,\phi))} \tag{2}$$

where $k = 2\pi/\lambda$ is the free-space wavenumber and $\hat{\mathbf{u}}(\theta, \phi)$ is the unit vector pointing in the observation direction [9, 10]

We define the steering vector as

$$\mathbf{d}(\theta, \phi) = \begin{bmatrix} e^{-jk\mathbf{r}_1 \cdot \hat{\mathbf{u}}(\theta,\phi)} & \cdots & e^{-jk\mathbf{r}_N \cdot \hat{\mathbf{u}}(\theta,\phi)} \end{bmatrix}^T, \tag{3}$$

where $\mathbf{d}(\theta, \phi) \in \mathbb{C}^N$, and the excitation vector $\mathbf{a} = [a_1, \ldots, a_N]^T$, the array factor can be compactly expressed as

$$AF(\theta, \phi) = \mathbf{d}^H(\theta, \phi), \mathbf{a}. \tag{4}$$

Importantly, for any fixed direction (θ, ϕ), the above array factor is affine in $\mathbf{a}$. This property allows linear equality and inequality constraints to be imposed, allowing convex formulations to follow, and this form will be used to build the QP, SOCP, and LP in following sections.

3 Hermitian Formulation of Radiation Performance

3.1 Quadratic Form of the Radiated Field

For a given direction, the radiation intensity is proportional to the squared magnitude of the electric field (1). Under the isotropic-element assumption ($E_e(\theta, \phi) = 1$), this reduces to

$$|E(\theta, \phi)|^2 = |AF(\theta, \phi)|^2 = |\mathbf{d}^H(\theta, \phi)\mathbf{a}|^2. \tag{5}$$

Using standard properties of complex vectors, this quantity can be written as a Hermitian quadratic form

$$|AF(\theta,\phi)|^2 = \mathbf{a}^H \mathbf{Q}(\theta,\phi)\mathbf{a}, \tag{6}$$

where

$$\mathbf{Q}(\theta,\phi) = \mathbf{d}(\theta,\phi)\mathbf{d}^H(\theta,\phi). \tag{7}$$

It follows immediately that $\mathbf{Q}$ is Hermitian since

$$\mathbf{Q}^H = (\mathbf{d}\mathbf{d}^H)^H = \mathbf{d}\mathbf{d}^H = \mathbf{Q}.$$

Moreover, for any $\mathbf{x} \in \mathbb{C}^N$,

$$\mathbf{x}^H \mathbf{Q}\mathbf{x} = \mathbf{x}^H \mathbf{d}\mathbf{d}^H \mathbf{x} = |\mathbf{d}^H \mathbf{x}|^2 \geq 0,$$

so $\mathbf{Q}(\theta,\phi) \succeq 0$ (positive semi-definite). From this, (6) is a convex quadratic function of $\mathbf{a}$, and upper bounds on it define convex constraints.

Additionally, since $\mathbf{Q}$ is the outer product of a nonzero vector with itself, its column space is $\text{span}\{\mathbf{d}(\theta,\phi)\}$ and therefore $\text{rank}(\mathbf{Q}) = 1$. $\mathbf{Q}(\theta,\phi)$ being Hermitian, positive semidefinite, and rank one allows the radiation pattern constraints to be expressed in forms that can be utilized for convex optimization.

3.2 Directivity as a Rayleigh Quotient

The directivity of an antenna array in a given direction (θ_0, ϕ_0) is defined as the ratio of the radiation intensity in that direction to the average radiation intensity over all directions. Under the Hermitian formulation, the directivity can be written as

$$D(\theta_0,\phi_0) = \frac{4\pi, \mathbf{a}^H \mathbf{Q}_0 \mathbf{a}}{\mathbf{a}^H \mathbf{P}\mathbf{a}}, \tag{8}$$

where $\mathbf{Q}_0 = \mathbf{Q}(\theta_0,\phi_0)$ and

$$\mathbf{P} = \int_\Omega \mathbf{Q}(\theta,\phi)\sin\theta, d\theta, d\phi \tag{9}$$

represents the total radiated power matrix. Both $\mathbf{Q}_0$ and $\mathbf{P}$ are Hermitian and positive definite, which ensures that the ratio above is well defined.

This expression has the form of a Rayleigh quotient, which can be cast in a quadratic optimization problem. Following [9], the maximization of directivity can be written as

$$\max_{\mathbf{a}} \frac{\mathbf{a}^H \mathbf{Q}_0 \mathbf{a}}{\mathbf{a}^H \mathbf{P}\mathbf{a}}, \tag{10}$$

which is equivalent to solving the generalized eigenvalue problem

$$\mathbf{Q}_0\mathbf{a} = \lambda \mathbf{P}\mathbf{a}. \tag{11}$$

The maximum achievable directivity corresponds to the largest eigenvalue $\lambda_{\max}$, and the optimal excitation vector is given by the associated eigenvector. This formulation provides the foundation for subsequent convex reformulations via quadratic and conic programming.

4 Convex Optimization Formulations

4.1 Quadratic Programming (QP)

Quadratic Programming (QP) is an optimization technique used to minimize a quadratic objective function subject to a set of linear inequality and equality constraints. The general

formulation of a quadratic optimization problem involving N_v decision variables, N_i inequality constraints, and N_e equality constraints is expressed as:

$$\min_{\vec{x}} \frac{1}{2}\vec{x}^T M\vec{x} + \vec{c}^T\vec{x} \tag{12}$$

$$\text{subject to } A\vec{x} < \vec{b} \tag{13}$$

$$A_{eq}\vec{x} = \vec{b}_{eq} \tag{14}$$

where $M \in \mathbb{R}^{N_v \times N_v}$ is a positive definite matrix representing the coefficients of the quadratic terms, $\vec{c} \in \mathbb{R}^{N_v}$ contains the coefficients for the linear terms, and $\vec{x} \in \mathbb{R}^{N_v}$ denotes the vector of optimization variables. The matrices $A \in \mathbb{R}^{N_i \times N_v}$ and $A_{eq} \in \mathbb{R}^{N_e \times N_v}$ define the inequality and equality constraints, respectively, with corresponding right-hand side vectors $\vec{b} \in \mathbb{R}^{N_i}$ and $\vec{b}_{eq} \in \mathbb{R}^{N_e}$. The physical interpretation of these parameters within the context of array optimization is detailed in the subsequent derivation.

4.2 QP Formulation for Antenna Array Optimization

Maximizing the directivity of an antenna array is equivalent to minimizing the total radiated power while maintaining a fixed radiation intensity in the desired look direction. Consequently, the directivity maximization problem can be formulated as:

$$\min_{\vec{a}} \vec{a}^\dagger P\vec{a} \tag{15}$$

$$\text{subject to } \vec{a}^\dagger Q_0\vec{a} = |\zeta|^2 \tag{16}$$

where $|\zeta|^2$ is a positive real constant chosen to fix the radiation intensity along the main beam direction. To cast this problem into a standard quadratic programming format, the quadratic constraint in (16) must be linearized. Instead of directly enforcing the intensity magnitude, we impose a constraint on the complex electric field, requiring it to match a specific complex-valued target. Since the intensity is given by:

$$|E(\theta_0,\phi_0)|^2 = \vec{a}^\dagger Q_0\vec{a} = \vec{a}^\dagger\vec{d}(\theta_0,\phi_0)\vec{d}(\theta_0,\phi_0)^\dagger\vec{a} = |\zeta|^2 \tag{17}$$

the magnitude of the electric field takes the form:

$$|E(\theta_0,\phi_0)| = |\vec{d}(\theta_0,\phi_0)^\dagger\vec{a}| = |\zeta| \tag{18}$$

Because the electric field is a complex quantity, this constraint can be decomposed into its real and imaginary components. Letting $\zeta = \zeta_R + j\zeta_I$, we obtain two independent linear constraints:

$$\begin{cases} \Re(E(\theta_0,\phi_0)) = \Re(\vec{d}(\theta_0,\phi_0)^\dagger\vec{a}) = \zeta_R \\ \Im(E(\theta_0,\phi_0)) = \Im(\vec{d}(\theta_0,\phi_0)^\dagger\vec{a}) = \zeta_I \end{cases} \tag{19}$$

where $\zeta_R, \zeta_I \in \mathbb{R}$. With this formulation, the field magnitude in the intended direction is fixed, effectively serving the same purpose as the original quadratic constraint, while the objective function minimizes the overall radiated power. Expanding the inner product term $\vec{d}(\theta_0,\phi_0)^\dagger\vec{a}$ yields:

$$\vec{d}(\theta_0,\phi_0)^\dagger\vec{a} = \Re(\vec{d}(\theta_0,\phi_0)^\dagger)\Re(\vec{a}) - \Im(\vec{d}(\theta_0,\phi_0)^\dagger)\Im(\vec{a}) + j[\Re(\vec{d}(\theta_0,\phi_0)^\dagger)\Im(\vec{a}) + \Im(\vec{d}(\theta_0,\phi_0)^\dagger)\Re(\vec{a})] \tag{20}$$

Substituting (20) into (19), the constraints are explicitly defined as:

$$\begin{cases} \Re(\vec{d}(\theta_0,\phi_0)^\dagger\vec{a}) = \Re(\vec{d}(\theta_0,\phi_0)^\dagger)\Re(\vec{a}) - \Im(\vec{d}(\theta_0,\phi_0)^\dagger)\Im(\vec{a}) \\ \Im(\vec{d}(\theta_0,\phi_0)^\dagger\vec{a}) = \Re(\vec{d}(\theta_0,\phi_0)^\dagger)\Im(\vec{a}) + \Im(\vec{d}(\theta_0,\phi_0)^\dagger)\Re(\vec{a}) \end{cases} \tag{21}$$

Accordingly, we define the real-valued extended vectors derived from the steering vector $\vec{d}(\theta_0, \phi_0)^\dagger$ as:

$$\begin{cases} \vec{d}_{0,R}^{\dagger} = [\Re(\vec{d}(\theta_0, \phi_0)^\dagger), -\Im(\vec{d}(\theta_0, \phi_0)^\dagger)] \\ \vec{d}_{0,I}^{\dagger} = [\Im(\vec{d}(\theta_0, \phi_0)^\dagger), +\Re(\vec{d}(\theta_0, \phi_0)^\dagger)] \end{cases} \tag{22}$$

To accommodate standard QP solvers which operate over real numbers, the complex optimization vector $\vec{a}$ is decomposed into $\vec{x} \in \mathbb{R}^{2N}$, comprising the real and imaginary parts:

$$\vec{x} = \begin{bmatrix} \Re(\vec{a}) \\ \Im(\vec{a}) \end{bmatrix} \tag{23}$$

Following a similar decomposition approach for the objective function, the term $\vec{a}^\dagger P \vec{a}$ is expanded as:

$$\vec{a}^\dagger P \vec{a} = \Re(\vec{a}^\dagger)\Re(P)\Re(\vec{a}) - \Im(\vec{a}^\dagger)\Re(P)\Im(\vec{a}) + j[-\Im(\vec{a}^\dagger)\Im(P)\Im(\vec{a}) + \Re(\vec{a}^\dagger)\Im(P)\Re(\vec{a})] \tag{24}$$

The real-valued extended matrices derived from matrix P are defined as:

$$\begin{cases} P_R = [\Re(P), -\Re(P)] \\ P_I = [\Im(P), -\Im(P)] \end{cases} \tag{25}$$

Therefore, the problem described in (25) can be expressed as a quadratic programming problem with linear equality constraints ($N_e = 2$, $N_i = 0$) in the form:

$$\min_{\vec{x}} \vec{x}^\dagger \begin{bmatrix} P_R \\ P_I \end{bmatrix} \vec{x} \tag{26}$$

$$\text{subject to } \vec{d}_{0,R}^{\dagger}\vec{x} = \zeta_R, \quad \vec{d}_{0,I}^{\dagger}\vec{x} = \zeta_I \tag{27}$$

From (26), it follows that nulls can be explicitly imposed in specific interference directions. Rather than using a quadratic power constraint for the nulls, we enforce a zero-field condition: $E(\theta_q, \phi_q) = 0$. The null-steering vector $\vec{d}(\theta_q, \phi_q)$ is decomposed into real and imaginary components similarly to the main beam vector, and (26) is reformulated to include these additional requirements:

$$\min_{\vec{x}} \vec{x}^\dagger \begin{bmatrix} P_R \\ P_I \end{bmatrix} \vec{x} \tag{28}$$

$$\text{subject to } \vec{d}_{0,R}^{\dagger}\vec{x} = \zeta_R, \quad \vec{d}_{0,I}^{\dagger}\vec{x} = \zeta_I, \quad \vec{d}_{q,R}^{\dagger}\vec{x} = 0, \quad \vec{d}_{q,I}^{\dagger}\vec{x} = 0 \tag{29}$$

This results in a QP problem with $N_i = 0$ and $N_e = 2 + 2\dim(\mathcal{Q})$, where $\dim(\mathcal{Q})$ represents the number of imposed nulls.

4.3 Second-Order Cone Programming (SOCP)

Here, we apply Second-Order Cone Programming (SOCP) for radiation pattern optimization. The objective is to maximize directivity in a specific direction while enforcing nulls in interference directions and limiting Sidelobe Levels (SLLs) within designated regions. SOCP problems minimize a linear objective function subject to a set of second-order cone constraints. The general formulation is given by:

$$\begin{aligned} &\min_{\vec{y}} \vec{f}^T \vec{y} \\ &\text{subject to } \|A_m \vec{y} + \vec{b}_m\| \leq \vec{c}_m^T \vec{y} + d_m, \quad m = 1, \ldots, N_i \\ &A_{eq}\vec{y} = \vec{b}_{eq} \end{aligned} \tag{30}$$

where N_i is the total number of inequality constraints, $\vec{y} \in \mathbb{R}^{N_v}$ is the optimization variable vector, and $\vec{f} \in \mathbb{R}^{N_v}$ defines the objective function. For each constraint m, the affine mapping is defined by the matrix A_m, vectors $\vec{b}_m, \vec{c}_m$, and scalar d_m. These constraints generalize the linear inequalities found in Linear Programming (LP) and QP by incorporating Euclidean norms. The equality constraints are defined by A_{eq} and $\vec{b}_{eq}$, consistent with the QP formulation.

The standard unit second-order cone (Lorentz cone) of dimension k is defined as:

$$\mathfrak{C}_k = \left\{ \begin{bmatrix} \vec{u} \\ t \end{bmatrix} \in \mathbb{R}^k \mid \vec{u} \in \mathbb{R}^{k-1}, t \in \mathbb{R}, \|\vec{u}\| \leq t \right\} \tag{31}$$

Ideally, a constraint corresponds to the inverse image of this unit cone under an affine mapping:

$$\begin{bmatrix} A_m \\ \vec{c}_m^T \end{bmatrix} \vec{y} + \begin{bmatrix} \vec{b}_m \\ d_m \end{bmatrix} \in \mathfrak{C}_{n_m} \tag{32}$$

where n_m is the dimension of the cone for the m-th constraint. Since the second-order cone is a convex set, SOCP is a convex optimization problem.

4.4 SOCP Formulation for Antenna Array Optimization

Directivity maximization in the SOCP framework begins with the quadratic form used in QP, $\vec{a}^\dagger P \vec{a}$. Since the matrix P is Hermitian positive definite, it admits a Cholesky decomposition $P = G^\dagger G$. Consequently, the quadratic term can be expressed as a squared Euclidean norm:

$$\vec{a}^\dagger P \vec{a} = \vec{a}^\dagger G^\dagger G \vec{a} = \|G\vec{a}\|^2 \tag{33}$$

Minimizing the squared norm is equivalent to minimizing the norm itself. Thus, the directivity maximization problem can be reformulated as:

$$\begin{aligned} &\min_{\vec{a}} \|G\vec{a}\| \\ &\text{subject to } \vec{a}^\dagger Q_0 \vec{a} = |\zeta|^2 \end{aligned} \tag{34}$$

To enable the use of standard solvers, the complex quantities $\vec{a}$ and G are decomposed into their real and imaginary components. The norm minimization then becomes:

$$\begin{aligned} &\min_{\vec{x}} \left\| \begin{bmatrix} G_R \\ G_I \end{bmatrix} \vec{x} \right\| \\ &\text{subject to } \vec{d}_{0,R}^\dagger \vec{x} = \zeta_R, \quad \vec{d}_{0,I}^\dagger \vec{x} = \zeta_I \end{aligned} \tag{35}$$

where $\vec{x} = [\Re(\vec{a})^T, \Im(\vec{a})^T]^T \in \mathbb{R}^{2N}$, and the matrices are defined as $G_R = [\Re(G), -\Im(G)]$ and $G_I = [\Im(G), +\Re(G)]$.

Standard SOCP requires a linear objective function. We therefore introduce an auxiliary scalar variable, δ, to bound the norm of the radiation vector, effectively transforming the objective into an epigraph form:

$$\|G\vec{a}\| \leq \delta \tag{36}$$

By minimizing δ, we minimize the norm. The problem is rewritten as:

$$\begin{aligned} &\min_{\delta} \delta \\ &\text{subject to } \left\| \begin{bmatrix} G_R \\ G_I \end{bmatrix} \vec{x} \right\| \leq \delta \\ &\vec{d}_{0,R}^\dagger \vec{x} = \zeta_R, \quad \vec{d}_{0,I}^\dagger \vec{x} = \zeta_I \end{aligned} \tag{37}$$

To align with the general SOCP form in (31), we define an augmented optimization vector $\vec{y} \in \mathbb{R}^{2N+1}$ that includes the auxiliary variable:

$$\vec{y} = \begin{bmatrix} \vec{x} \\ \delta \end{bmatrix}, \quad \vec{f} = [0, \ldots, 0, 1]^T \in \mathbb{R}^{2N+1} \tag{38}$$

such that the objective function becomes $\delta = \vec{f}^T \vec{y}$. The matrices and vectors must be augmented with zeros to account for the dimensionality increase:

$$\tilde{G}_R = [G_R \quad 0], \quad \tilde{G}_I = [G_I \quad 0], \quad \tilde{d}_{0,R} = \begin{bmatrix} \vec{d}_{0,R} \\ 0 \end{bmatrix}, \quad \tilde{d}_{0,I} = \begin{bmatrix} \vec{d}_{0,I} \\ 0 \end{bmatrix}. \tag{39}$$

The basic problem is now expressed as:

$$\begin{aligned} &\min_{\vec{y}} \vec{f}^T \vec{y} \\ &\text{subject to } \left\| \begin{bmatrix} \tilde{G}_R \\ \tilde{G}_I \end{bmatrix} \vec{y} \right\| \leq \vec{f}^T \vec{y} \\ &\tilde{d}_{0,R}^\dagger \vec{y} = \zeta_R, \quad \tilde{d}_{0,I}^\dagger \vec{y} = \zeta_I \end{aligned} \tag{40}$$

While null steering is handled via linear equality constraints (as in QP), suppressing Sidelobe Levels (SLLs) requires inequality constraints on the field magnitude. We require that the magnitude of the electric field in a defined region $\mathcal{M}$ does not exceed a threshold T_m relative to the main beam magnitude:

$$|E(\theta_m, \phi_m)| \leq T_m |E(\theta_0, \phi_0)| \tag{41}$$

where $T_m = 10^{-SLL_m/20}$ and SLL_m is the required attenuation in dB. Since the main beam magnitude is fixed at $\sqrt{\zeta_R^2 + \zeta_I^2}$, and the field magnitude corresponds to the Euclidean norm of the complex steering vector product, this constraint is convex and fits the SOCP form:

$$\left\| \begin{bmatrix} \tilde{d}_{m,R}^\dagger \\ \tilde{d}_{m,I}^\dagger \end{bmatrix} \vec{y} \right\| \leq T_m \sqrt{\zeta_R^2 + \zeta_I^2} \tag{42}$$

Here, the augmented steering vectors $\tilde{d}_{m,R}$ and $\tilde{d}_{m,I}$ for direction (θ_m, ϕ_m) are defined similarly to (41).

Combining these elements, the complete SOCP formulation for maximizing directivity with null steering and SLL control is:

$$\begin{aligned} &\min_{\vec{y}} \vec{f}^T \vec{y} \\ &\text{subject to } \left\| \begin{bmatrix} \tilde{G}_R \\ \tilde{G}_I \end{bmatrix} \vec{y} \right\| \leq \vec{f}^T \vec{y} \\ &\left\| \begin{bmatrix} \tilde{d}_{m,R}^\dagger \\ \tilde{d}_{m,I}^\dagger \end{bmatrix} \vec{y} \right\| \leq T_m \sqrt{\zeta_R^2 + \zeta_I^2}, \quad \forall (\theta_m, \phi_m) \in \mathcal{M} \\ &\tilde{d}_{0,R}^\dagger \vec{y} = \zeta_R, \quad \tilde{d}_{0,I}^\dagger \vec{y} = \zeta_I \\ &\tilde{d}_{q,R}^\dagger \vec{y} = 0, \quad \tilde{d}_{q,I}^\dagger \vec{y} = 0, \quad \forall (\theta_q, \phi_q) \in \mathcal{Q} \end{aligned} \tag{43}$$

This problem has $N_v = 2N + 1$ variables, $N_e = 2 + 2\dim(\mathcal{Q})$ equality constraints, and $N_i = 1 + \dim(\mathcal{M})$ cone constraints.

4.5 LP Formulation for SLL Minimization

In contrast to QP and SOCP, the Linear Programming (LP) formulation does not optimize array directivity directly. Instead, it adopts a minimax perspective, seeking to minimize the maximum Sidelobe Level (SLL) over a specified angular region. This formulation is particularly attractive in scenarios where sidelobe suppression is the primary design objective and computational efficiency is paramount.

To enable the use of Linear Programming, the quadratic constraint on the field magnitude used in SOCP ($|E| \leq \delta$) must be relaxed into linear constraints. Geometrically, this involves approximating the circular constraint region in the complex plane with a square. While this leads to a slightly conservative approximation compared to SOCP, it allows for the use of simplex or interior-point LP algorithms, which are highly scalable and robust.

The magnitude of the complex electric field at an angle (θ_m, ϕ_m) is bounded by the sum of the magnitudes of its components (triangle inequality):

$$|E(\theta_m,\phi_m)| = |\Re\{E(\theta_m,\phi_m)\} + j\Im\{E(\theta_m,\phi_m)\}| \leq |\Re\{E(\theta_m,\phi_m)\}| + |\Im\{E(\theta_m,\phi_m)\}| \quad (44)$$

To strictly linearize the problem, we enforce separate bounds on the real and imaginary components. We introduce the auxiliary variable δ and impose that both components must effectively lie within a box of size 2δ centered at the origin:

$$|\Re\{E(\theta_m,\phi_m)\}| \leq \delta, \quad |\Im\{E(\theta_m,\phi_m)\}| \leq \delta, \quad \forall(\theta_m,\phi_m) \in \mathcal{M} \quad (45)$$

Unlike the SOCP formulation, where δ bounded the total radiated power (Euclidean norm), here δ represents the maximum amplitude of the field components in the sidelobe region (Infinity norm). The goal is to minimize this maximum value. The resulting linear optimization problem is formulated as:

$$\begin{aligned}
&\min_{\delta} \delta \\
&\text{subject to} \\
&|\Re\{E(\theta_m,\phi_m)\}| \leq \delta, \quad \forall(\theta_m,\phi_m) \in \mathcal{M} \\
&|\Im\{E(\theta_m,\phi_m)\}| \leq \delta, \quad \forall(\theta_m,\phi_m) \in \mathcal{M} \\
&\Re\{E(\theta_0,\phi_0)\} = \zeta_R \\
&\Im\{E(\theta_0,\phi_0)\} = \zeta_I
\end{aligned} \quad (46)$$

Using the augmented variable vector $\vec{y} = [\vec{x}^T, \delta]^T$ and the objective vector $\vec{f} = [0, \ldots, 0, 1]^T$ defined previously, the absolute value constraints can be rewritten in terms of the linear cost function $\delta = \vec{f}^T\vec{y}$:

$$\begin{aligned}
&\min_{\vec{y}} \vec{f}^T\vec{y} \\
&\text{subject to} \\
&|\vec{d}^{\dagger}_{m,R}\vec{y}| \leq \vec{f}^T\vec{y} \\
&|\vec{d}^{\dagger}_{m,I}\vec{y}| \leq \vec{f}^T\vec{y} \\
&\vec{d}^{\dagger}_{0,R}\vec{y} = \zeta_R \\
&\vec{d}^{\dagger}_{0,I}\vec{y} = \zeta_I
\end{aligned} \quad (47)$$

Since the condition $|u| \leq \delta$ is mathematically equivalent to the pair of linear inequalities $u \leq \delta$ and $-u \leq \delta$, each constraint in (56) expands into two linear inequalities. This expansion allows the problem to be expressed in standard LP form:

$$\begin{aligned}
\vec{d}^{\dagger}_{m,R}\vec{y} \leq \vec{f}^T\vec{y}, \quad \vec{d}^{\dagger}_{m,I}\vec{y} \leq \vec{f}^T\vec{y}, \\
-\vec{d}^{\dagger}_{m,R}\vec{y} \leq \vec{f}^T\vec{y}, \quad -\vec{d}^{\dagger}_{m,I}\vec{y} \leq \vec{f}^T\vec{y}.
\end{aligned} \quad (48)$$

Rearranging terms to isolate the decision variables on the left-hand side yields the final Linear Programming formulation:

$$
\begin{aligned}
&\min_{\vec{y}} \vec{f}^T \vec{y} \\
&\text{subject to} \\
&(\vec{d}^{\dagger}_{m,R} - \vec{f}^T)\vec{y} \leq 0 \\
&(-\vec{d}^{\dagger}_{m,R} - \vec{f}^T)\vec{y} \leq 0 \\
&(\vec{d}^{\dagger}_{m,I} - \vec{f}^T)\vec{y} \leq 0 \\
&(-\vec{d}^{\dagger}_{m,I} - \vec{f}^T)\vec{y} \leq 0 \\
&\vec{d}^{\dagger}_{0,R}\vec{y} = \zeta_R \\
&\vec{d}^{\dagger}_{0,I}\vec{y} = \zeta_I
\end{aligned}
\tag{49}
$$

This formulation is entirely linear in both the objective and the constraints. Although it does not allow for a specific pre-defined SLL threshold to be set as a hard constraint, it finds the optimal excitation that minimizes the peak sidelobe level in the minimax sense.

5 Results and Discussion

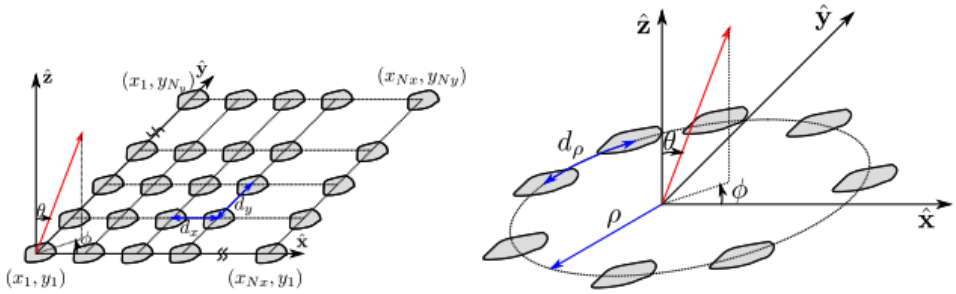

Figure 1: Antenna array configuration, rectangular (left), and circular (right) [9].

5.1 QP: Optimal Directivity with Null Requirements

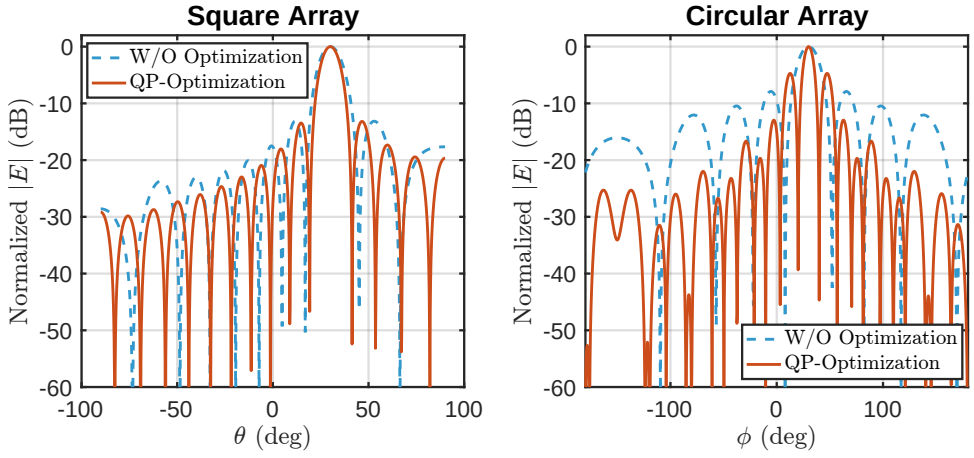

Figure 2: Radiation pattern for the QP-based optimization maximizing directivity.

Simulation Setup

The QP-based convex optimization framework is verified through numerical case studies on two distinct geometries: a square array and a circular array. The square array consists of a 16×16 element configuration on a uniform grid with inter-element spacing of $0.3\lambda_0$, as illustrated in Figure 1. The circular array comprises 32 elements distributed along a radius $\rho = \lambda_0$ with an arc separation of $d_\rho = 0.9\lambda_c$. For consistency, isotropic elements are assumed, and the Array Factor (AF) is calculated directly. The steering directions were fixed at $(\theta_0, \phi_0) = (30°, 0°)$ for the square array and $(90°, 30°)$ for the circular array.

Directivity Maximization

Figure 2 compares the normalized radiation patterns of the classical phase-shifted approach against the QP-optimized solution. For the square array, the classical excitation already provides a near-optimal directivity, closely matching the analytical reference. Consequently, the QP optimization yields a nearly identical pattern, with only negligible variations in the side lobe levels (SLL).

The impact of optimization is much more pronounced for the circular array. The conventional phase-shift method suffers from high side lobes due to the array's sparse, non-uniform geometry. The QP optimization effectively compensates for this, suppressing the side lobes significantly (by approximately 10 dB) and shaping the main beam to approximate an ideal directive pattern more closely.

Null Steering Capabilities

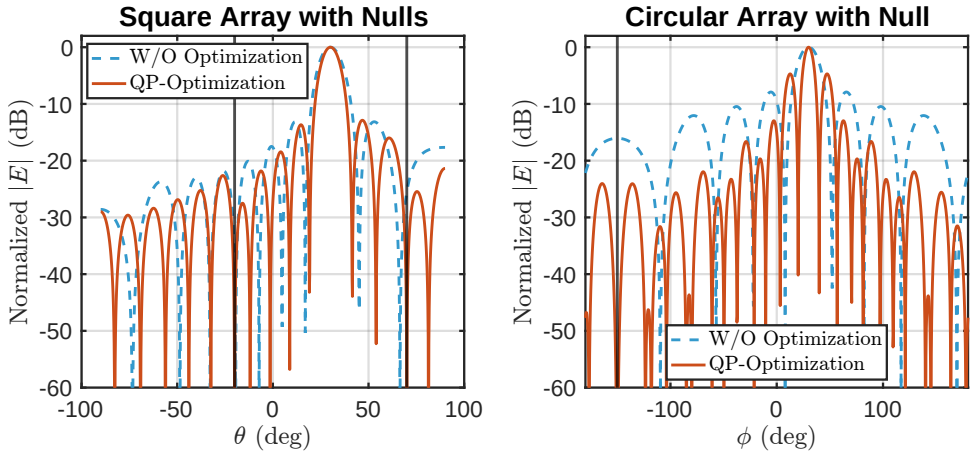

Figure 3: Radiation pattern for the QP-based optimization maximizing directivity and placing nulls.

To demonstrate the flexibility of the proposed method, we incorporated null constraints into the directivity maximization problem. We enforced nulls at $\theta \in \{-20°, 70°\}$ for the square array and $\phi = -150°$ for the circular array. As shown in Figure 3, the optimization successfully synthesizes deep nulls (reaching depths below -50 dB) at the prescribed angles without significantly degrading the main beam gain or the overall pattern shape compared to the unconstrained case.

Excitation Coefficients

Figure 4 visualizes the element excitations corresponding to the null-steering scenario. The "Classic" weights (represented by diamonds) generally exhibit uniform magnitude with varying phases. In contrast, the "Optimized" weights (circles) show a redistribution in the complex

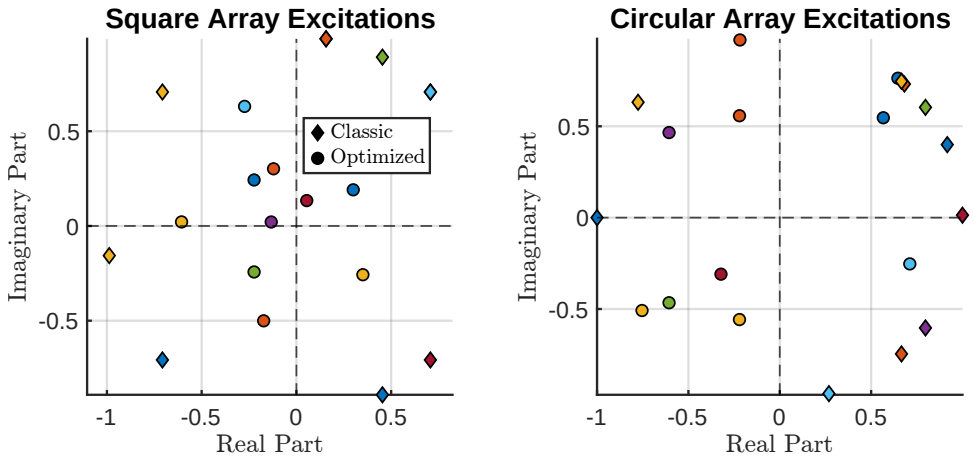

Figure 4: Excitation coefficients for the square and circular arrays for the QP-based optimization with null directions. Each color corresponds to an element.

plane. Notably, the optimized coefficients exhibit distinct amplitude tapering—indicated by points moving inward from the unit circle. This demonstrates that the solver modulates both the magnitude and phase of each element to satisfy the strict null constraints while maintaining high directivity.

5.2 SOCP: Maximizing Directivity, Null Requirements, and SLL Reduction

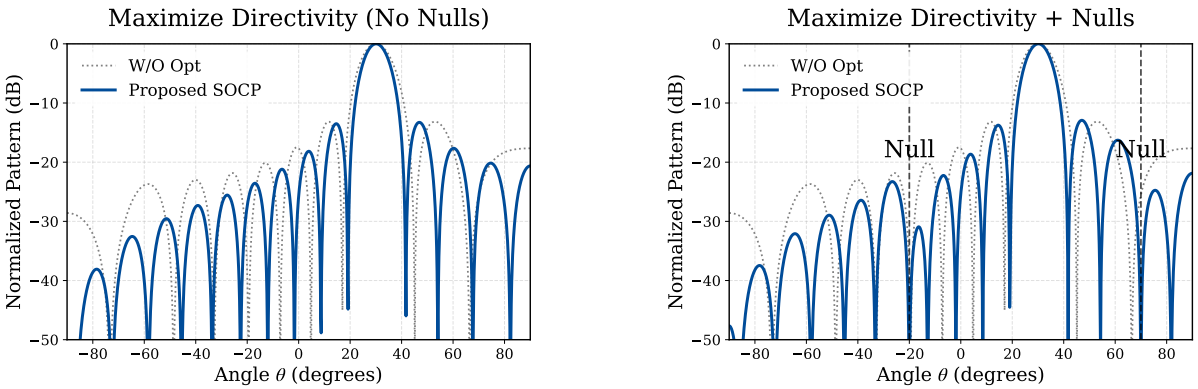

(a) Maximize directivity

(b) Maximize directivity with nulls

Figure 5: Radiation pattern of the **square array** for the SOCP-based optimization.

Directivity Maximization and Nulls

Building on the previously described square array geometry, three distinct optimization strategies were evaluated using Second-Order Cone Programming (SOCP). The first two scenarios mirror standard Quadratic Programming (QP) approaches: the first sought solely to maximize directivity, while the second supplemented this objective with null steering constraints. For the square array, nulls were enforced at angles $\theta_1 = -20°$ and $\theta_2 = 70°$. Figure 5 displays the resulting radiation patterns for these two cases. The results are analogous to classic maximum directivity excitations, with the second case successfully synthesizing deep nulls in the specified directions. As expected, these initial SOCP results closely resemble those achievable with standard QP formulations.

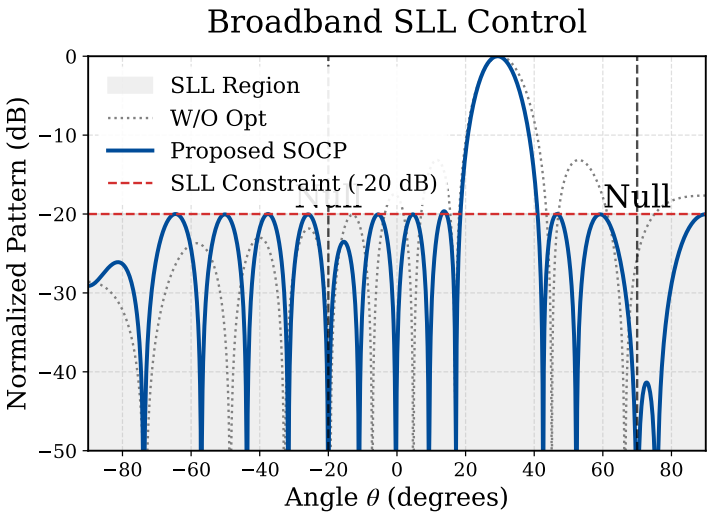

Figure 6: Radiation pattern of the **square array** for the SOCP-based optimization **maximizing directivity, forcing nulls, and reducing SLL level**.

Incorporating Sidelobe Level (SLL) Reduction

The primary advantage of SOCP, however, lies in its ability to incorporate stringent Sidelobe Level (SLL) reduction constraints alongside directivity maximization and null steering. This is demonstrated in the third square array optimization case shown in Figure 6. Here, in addition to maximizing directivity in the pointing direction and enforcing the previously defined nulls, a quadratic constraint, referencing equation (48), was introduced to limit the SLL. The resulting pattern maintains a highly directive main beam and the required nulls, while successfully suppressing all sidelobes to below a -20 dB threshold across the entire angular range.

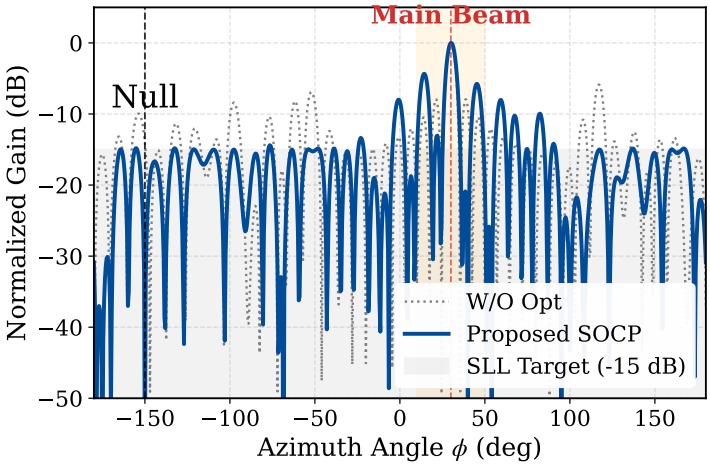

Figure 7: Radiation pattern of the **circular array** with SOCP-based optimization imposing SLL requirements and nulls.

SOCP Optimization for Circular Array

Finally, this comprehensive SOCP optimization strategy, combining directivity maximization, null forcing, and SLL reduction, was applied to the circular array geometry. A null was imposed at $\phi = -150^\circ$ (consistent with prior QP comparison cases), and an SLL constraint of -15 dB was enforced. While previous QP approaches significantly improved directivity compared to

uniform excitations, they often resulted in impractically high first sidelobes (exceeding -10 dB). The SOCP results presented in Figure 7 demonstrate that a highly collimated beam can be achieved while simultaneously satisfying the null condition and drastically reducing adjacent sidelobes to meet the target -15 dB specification.

5.3 LP: SLL Reduction

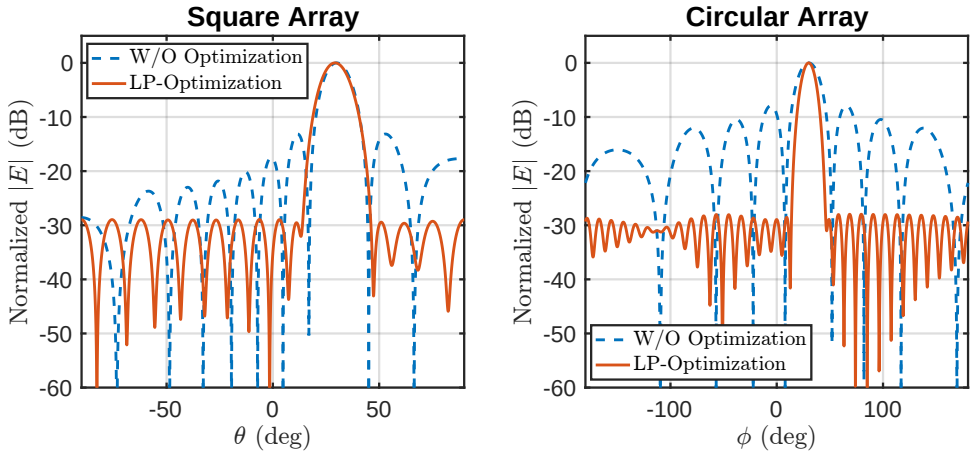

Figure 8: Radiation pattern for the LP-based optimization for reducing SLLs.

For the Linear Programming (LP) optimization, the primary objective was to minimize the Sidelobe Levels (SLL) outside the main beam. Figure 8 presents a comparison of the radiation patterns for the square and circular arrays, contrasting the LP-optimized results against the unoptimized (classic excitation) baselines.

In the case of the square array, the optimization successfully suppressed the SLL to below -30 dB across the entire angular spectrum, representing a significant improvement over the classic excitation. Similarly, for the circular array, the LP formulation achieved SLL suppression below -30 dB throughout the entire visible range $\phi \in [-180°, 180°]$. This result demonstrates that the LP approach not only drastically reduces the SLL compared to the classic excitation but also maintains a focused main beam around the pointing direction $(\theta_0, \phi_0) = (90°, 30°)$.

6 Conclusion

In this project, we studied antenna array pattern synthesis through convex optimization, grounding the formulation in the techniques and principles derived from the material in ENEE662. By expressing the radiation pattern of the array in quadratic Hermitian form, we demonstrated that classical antenna design problems can be systematically reformulated as convex optimization problems, specifically Quadratic Programming (QP), Second-Order Cone Programming (SOCP), and Linear Programming (LP).

The QP form demonstrated that directivity maximization, with optional null placement, can be solved efficiently and be globally optimal, offering an alternative to phase-only steering and optimization methods. SOCP further extended this by incorporating SLL constraints. This allowed for simultaneous control of directivity, null placement, and sidelobe suppression, which are difficult to implement on QP alone. Finally, the LP offered an efficient minimax approach to the SLL reduction, demonstrating how conservative convex forms can still give meaningful improvements when directivity optimization is not the main goal of optimization.

Across the three formulations, numerical examples confirmed that the method of convex optimization is a viable and efficient approach for antenna array analysis. This work shows how these physical problems can be mapped into convex sets and objective functions, and showing a

practical application of convex optimization theory. These methods are particularly well suited for applications in adaptive beamforming, interference suppression, and antenna array design, where flexibility and optimality are chief requirements.

Data Availability

The codes for this study are available at this Github repository.

References

[1] J. Hasch, E. Topak, R. Schnabel, T. Zwick, R. Weigel, and C. Waldschmidt, "Millimeter-wave technology for automotive radar sensors in the 77 ghz frequency band," *IEEE transactions on microwave theory and techniques*, vol. 60, no. 3, pp. 845–860, 2012.

[2] F. Liu, Y. Cui, C. Masouros, J. Xu, T. X. Han, Y. C. Eldar, and S. Buzzi, "Integrated sensing and communications: Toward dual-functional wireless networks for 6g and beyond," *IEEE journal on selected areas in communications*, vol. 40, no. 6, pp. 1728–1767, 2022.

[3] E. G. Larsson, O. Edfors, F. Tufvesson, and T. L. Marzetta, "Massive mimo for next generation wireless systems," *IEEE communications magazine*, vol. 52, no. 2, pp. 186–195, 2014.

[4] O. Bulatsyk, B. Z. Katsenelenbaum, Y. P. Topolyuk, and N. N. Voitovich, *Phase optimization problems: Applications in wave field theory*. John Wiley & Sons, 2010.

[5] F. J. Ares-Pena, J. A. Rodriguez-Gonzalez, E. Villanueva-Lopez, and S. Rengarajan, "Genetic algorithms in the design and optimization of antenna array patterns," *IEEE Transactions on Antennas and Propagation*, vol. 47, no. 3, pp. 506–510, 1999.

[6] M. Donelli, A. Martini, and A. Massa, "A hybrid approach based on pso and hadamard difference sets for the synthesis of square thinned arrays," *IEEE Transactions on Antennas and Propagation*, vol. 57, no. 8, pp. 2491–2495, 2009.

[7] J. Li, Y. Liu, W. Zhao, and T. Zhu, "Application of dandelion optimization algorithm in pattern synthesis of linear antenna arrays," *Mathematics*, vol. 12, no. 7, p. 1111, 2024.

[8] S. Boyd and L. Vandenberghe, *Convex optimization*. Cambridge university press, 2004.

[9] Á. F. Vaquero and J. Córcoles, "Convex formulations for antenna array pattern optimization through linear, quadratic, and second-order cone programming," *Mathematics*, vol. 13, no. 11, p. 1796, 2025.

[10] C. A. Balanis, *Antenna Theory: Analysis and Design*, 3rd ed. Hoboken, NJ: John Wiley & Sons, 2005.